Laser Phys. **23** (2013) 105811 (7pp) doi:10.1088/1054-660X/23/10/105811

Spectroscopic characterization and pulsed laser operation of Eu^{3+}:$KGd(WO_4)_2$ crystal

P A Loiko[1], V I Dashkevich[2], S N Bagaev[3], V A Orlovich[2], A S Yasukevich[1], K V Yumashev[1], N V Kuleshov[1], E B Dunina[4], A A Kornienko[4], S M Vatnik[3] and A A Pavlyuk[5]

[1] Center for Optical Materials and Technologies, Belarusian National Technical University, 65/17 Nezavisimosti Avenue, Minsk, 220013, Belarus
[2] B I Stepanov Institute of Physics, National Academy of Sciences of Belarus, 68 Nezavisimosti Avenue, Minsk, 220072, Belarus
[3] Institute of Laser Physics, Siberian Branch of Russian Academy of Sciences, 13/3 Lavrentyev Avenue, Novosibirsk, 630090, Russia
[4] Vitebsk State Technological University, 72 Moskovskaya Avenue, Vitebsk, 210035, Belarus
[5] A V Nikolaev Institute of Inorganic Chemistry, Siberian Branch of Russian Academy of Sciences, 3 Lavrentyev Avenue, Novosibirsk, 630090, Russia

E-mail: kinetic@tut.by (P A Loiko)

Received 3 July 2013, in final form 3 August 2013
Accepted for publication 5 August 2013
Published 22 August 2013
Online at stacks.iop.org/LP/23/105811

Abstract
Europium-doped monoclinic potassium gadolinium tungstate $KGd(WO_4)_2$ crystals are grown by the top-seeded solution growth (TSSG) technique. Their absorption spectra are studied in detail for principal light polarizations, $\boldsymbol{E} \parallel N_p$, N_m and N_g. It is accompanied by determination of absorption oscillator strengths by means of the theory of f–f transition intensities for systems with anomalously strong configuration interaction. Spectral and temporal characteristics of luminescence associated with $^5D_0 \rightarrow {}^7F_J$ transitions are analyzed, and luminescence branching ratios and the radiative lifetime of the $^5D_0$ state are determined. Stimulated-emission cross-section spectra are evaluated for Eu:$KGd(WO_4)_2$ crystal. Pulsed Eu:$KGd(WO_4)_2$ lasers operating at room temperature at the wavelength of 702.8 nm ($^5D_0 \rightarrow {}^7F_4$ transition) are studied at Eu concentration of 10/25 at.%. Under laser pumping at 533.6 nm, a maximum output energy of 570 μJ is obtained. The main limitation for laser operation at $^5D_0 \rightarrow {}^7F_2$ transition is strong excited-state absorption via the $^5D_0 \rightarrow {}^5F_4$ channel.

(Some figures may appear in colour only in the online journal)

1. Introduction

Trivalent europium ions, Eu^{3+}, are characterized by intense red luminescence associated with $^5D_0 \rightarrow {}^7F_2$ transition within a $4f^6$ electronic shell (centered at ~612 nm). Eu^{3+}-doped red phosphors are used in tricolor fluorescent lamps, field emission displays and solid-state lightning. Widespread hosts for Eu^{3+} are yttrium oxide Y_2O_3 (as nanocrystallites [1] or thin films [2]), and gallium nitride GaN [3, 4]. Laser action with Eu^{3+} was realized for the first time in [5, 6] under cryogenic temperatures; bulk Y_2O_3 and liquid chelate were used as host materials. Room-temperature (RT) lasing was obtained with Eu:GaN [7] and Eu:polymer [8] thin films.

Recently, the family of Eu-doped laser-active materials was extended by potassium gadolinium double tungstate, namely Eu(25 at.%):$KGd(WO_4)_2$ [9]. Pulsed lasing was obtained at ~703 nm (due to the $^5D_0 \rightarrow {}^7F_4$ transition); a frequency-doubled Nd:$KGd(WO_4)_2$ laser was used as a pump source. Yb- and Tm-doped double tungstates (DTs), $KRE(WO_4)_2$ (RE = Gd, Y, Lu) are

well-recognized materials for high-efficiency diode-pumped solid-state lasers [10, 11]. These crystals offer high rare-earth dopant concentrations and intense and wide bands in polarized absorption and stimulated-emission spectra. Thus, further investigation of spectroscopic and laser properties of Eu:DTs is rather interesting. Spectroscopic characterization of $KLu(WO_4)_2$ doped with Eu^{3+}(0.5–5 at.%) was recently performed in [12]. Nanocrystalline phosphors Eu:$KGd(WO_4)_2$, Eu:$KYb(WO_4)_2$, $KEu(WO_4)_2$ and Eu:$KGd(W/MoO_4)_2$ were also studied [13–17].

From the point of matching of rare-earth ionic radii, $KGd(WO_4)_2$ is the best choice for Eu doping among the DT family. Indeed, ionic radii for eight-fold coordinated Gd^{3+} and Eu^{3+} are 1.053 and 1.066 Å (compare with 0.977 Å for Lu^{3+}). Thus, in the present paper we perform detailed spectroscopic investigation of highly doped Eu:$KGd(WO_4)_2$. In addition, a comparative study of pulsed Eu(10 at.%): and Eu(25 at.%):$KGd(WO_4)_2$ lasers operating at the $^5D_0 \rightarrow {}^7F_4$ transition is presented.

2. Experimental details

Eu:$KGd(WO_4)_2$, Eu:KGdW, crystals were grown by a top-seeded solution growth method (TSSG) with pulling (the temperature of polymorphic phase transition to the monoclinic phase [18] was 1010 °C); potassium ditungstate $K_2W_2O_7$ was used as a solvent. The growth was performed under low thermal gradients, <0.1 °C cm^{-1} [19]. Seed crystals were oriented along the ***b***, [010], crystallographic axis. The content of Eu^{3+} ions was 10 at.% or 25 at.% ($N_{Eu} = 6.09$ or 15.3×10^{-20} cm^3, the crystal density $\rho = 7.049$ g cm^{-3}); and the growth rate was 5–7 and 3 mm d^{-1}, accordingly. Large-volume crystal boules (~60 mm in length, with a ~20 mm × 20 mm edge) thus obtained were free of cracks and inclusions. The crystals had weak rose coloration.

For spectroscopic studies, two polished plates with dimensions $5(N_p) \times 5(N_m) \times 2(N_g)$ and $5(N_g) \times 5(N_m) \times 2(N_p)$ mm^3 were cut from an Eu(10 at.%):KGdW crystal boule. Polarized absorption spectra in the UV, visible (350–640 nm) and near-IR (1.8–2.9 μm) were measured with a Varian CARY 5000 spectrophotometer; spectral bandwidth (SBW) was 0.15 nm. Luminescence was excited by focused radiation of 402 nm InGaN laser diode (its cw output power was 50 mW). It was collected in the direction perpendicular to the direction of pump light propagation by a wide-aperture lens. The spectrum was registered by means of a lock-in amplifier and monochromator MDR-23 (SBW ~ 0.5 nm) with a Hamamatsu C5460-01 photodetector attached to its output slit. A Glan–Taylor polarizer was inserted before the input slit of the monochromator.

For investigation of luminescence decay, focused output radiation of optical parametric oscillator (OPO) Lotis TII LT-2214 was used as an excitation source ($\lambda_{exc} = 534$ nm). OPO was pumped by a flashlamp-pumped *Q*-switched Nd:YAG laser with third harmonic generation. The duration of the excitation pulse was ~20 ns. Luminescence was collected by a wide-aperture lens and re-imaged to the input slit of monochromator MDR-12; it was then detected with a Hamamatsu C5460 photodetector (40 ns response time) and a 500 MHz Textronix TDS-3052B digital oscilloscope.

In laser experiments, Eu:KGdW crystals were longitudinally pumped by the second harmonic (SH) of a *Q*-switched flashlamp-pumped Nd:KGdW laser. The SH pulse energy was varied in the range of 1–37 mJ by changing the flashlamp pump energy (the duration of the SH pulse was 45–7 ns, accordingly). The energy of the output laser pulse was measured with PE50-DIF and PE9-SH sensors. A BeamON IR1550 CCD camera was used to capture the spatial profile of the output beam for Eu:KGdW lasers.

3. Results and discussion

3.1. Optical absorption

The detailed structure of polarized absorption bands of Eu^{3+} ions in KGdW crystal is presented in figure 1. Spectral bands in the visible (390–620 nm) are related to transitions from lower-lying $^7F_{0-2}$ states to $^5D_{0-3}$ and $^5L_6$ excited states. Clearly resolved transitions from $^7F_1$ and $^7F_2$ states are related to their efficient thermal population (corresponding probabilities are 0.33 and 0.02, compared with 0.65 for $^7F_0$). The most intense band corresponds to $^7F_0 \rightarrow {}^7F_6$ transition (centered at 394.7 nm, with peak absorption coefficient ~20 cm^{-1} for $\boldsymbol{E} \parallel N_p$ and N_m). The attribution of bands in figure 1 is similar to one presented in [20] for Eu:$Y_3Ga_5O_{12}$. Characteristic bands of Eu^{3+} in the near-IR (related to transitions between ^7F_J states) are also detected for Eu:KGdW (see figure 1). They span the 1.8–2.8 μm range, up to the absorption bands of OH-groups (near 3 μm).

Most interesting from the point of laser pumping is the band associated with the $^7F_1 \rightarrow {}^5D_1$ transition. Its detailed analysis is presented in table 1. Here λ_{peak} is the peak wavelength, and σ_{abs} is the corresponding peak absorption cross-section. Like other rare-earth-doped DTs, Eu:KGdW is characterized by profound anisotropy of optical absorption: max. σ_{abs} corresponds to light polarization $\boldsymbol{E} \parallel N_m$, σ_{abs} for $\boldsymbol{E} \parallel N_p$ takes intermediate place, while $\boldsymbol{E} \parallel N_g$ is almost not suitable for pumping. Indeed, at $\lambda_{peak} = 534.3$ nm, $\sigma_{abs}(m):\sigma_{abs}(p):\sigma_{abs}(g) = 6.8:1.7:1$. The anisotropy appears not only in the intensity of absorption peaks, but also in their position. Indeed, the discussed band for $\boldsymbol{E} \parallel N_p$ consists of three peaks (centered at 534.3, 538.6 and 539.5 nm), while for $\boldsymbol{E} \parallel N_m$ and N_g the second peak is missing.

From figure 1 and table 1, it is clear that laser pumping should be performed into the 534.3 nm peak for $\boldsymbol{E} \parallel N_m$ (in order to get access to high pumping efficiency). The main problem here is still the moderate peak absorption ($\sigma_{abs} = 0.89 \times 10^{-20}$ cm^2, or 5.45 cm^{-1} for Eu(10 at.%)-doping) and small full width at half maximum (FWHM) for this peak (~0.6 nm).

The UV absorption edge for Eu:KGdW crystal is positioned at 280 ± 5 nm ($E_g = 4.4 \pm 0.1$ eV), close to the data for pure KGdW crystal. The UV region of the absorption spectrum for Eu:KGdW is enriched by peaks that are related to transitions from $^7F_{0,1}$ states to higher-lying excited states, ^5L_J, ^5G_J, ^5D_J (see figure 2 for an overview of the absorption

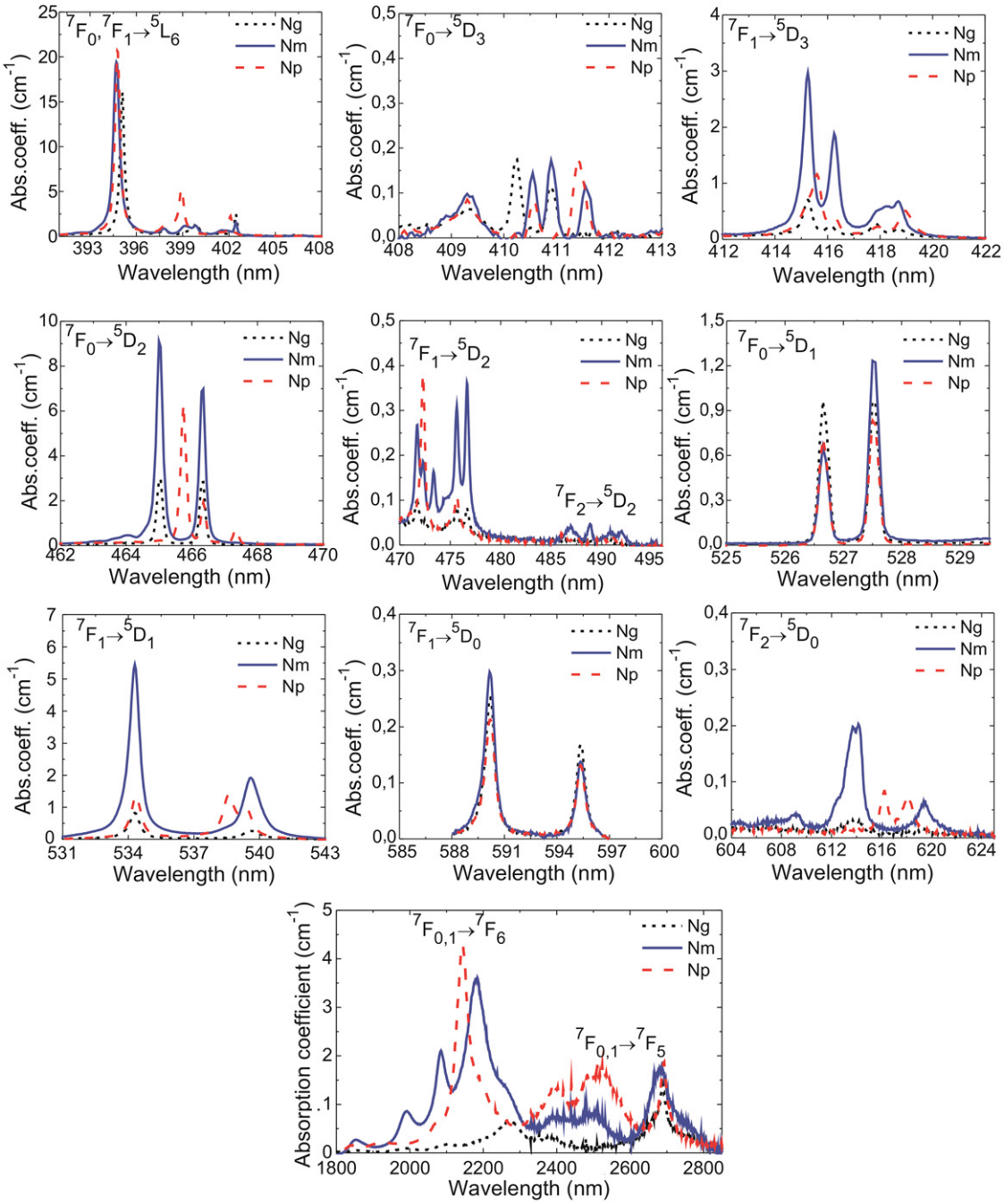

Figure 1. Detailed structure of polarized absorption bands for the Eu(10 at.%):KGd$(WO_4)_2$ crystal.

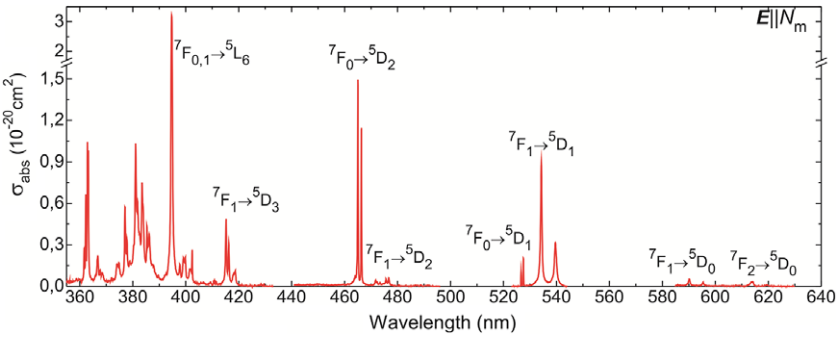

Figure 2. Absorption spectrum of Eu:KGd$(WO_4)_2$ crystal in the visible for light polarization $\boldsymbol{E} \parallel N_m$.

Table 1. Anisotropy of absorption and stimulated-emission cross-sections for Eu^{3+} ions in $KGd(WO_4)_2$ crystal.

Absorption			
Transition[a]	Polarization	λ_{peak} (nm)	σ_{abs} (10^{-20} cm^2)
$^7F_1 \rightarrow {}^5D_1$	$\boldsymbol{E} \parallel N_p$	534.3	0.22
		538.6	0.23
		539.5	0.15
	$\boldsymbol{E} \parallel N_m$	534.3	0.89
		539.5	0.31
	$\boldsymbol{E} \parallel N_g$	534.3	0.13
		539.5	0.04
Stimulated emission			
Transition[a]	Polarization	λ_{peak} (nm)	σ_{em} (10^{-20} cm^2)
$^5D_0 \rightarrow {}^7F_2$	$\boldsymbol{E} \parallel N_p$	617.6	1.35
		615.7	1.22
	$\boldsymbol{E} \parallel N_m$	613.6	2.78
		618.9	1.59
	$\boldsymbol{E} \parallel N_g$	613.6	0.44
		618.9	0.29
$^5D_0 \rightarrow {}^7F_4$	$\boldsymbol{E} \parallel N_p$	703.5	2.34
	$\boldsymbol{E} \parallel N_m$	702.1	3.02
		705.2	1.69
	$\boldsymbol{E} \parallel N_g$	702.1	0.38
		705.2	0.95

[a] Transitions interesting for laser operation are considered.

Table 2. Polarization-averaged absorption oscillator strengths for Eu^{3+} ions in $KGd(WO_4)_2$ crystal. (Note: $\langle f_{exp}\rangle$—as determined from absorption spectra; $\langle f_{asci}\rangle$—as calculated by the theory of f–f transition intensities for systems with anomalously strong configuration interaction; all f values were averaged over light polarizations $\boldsymbol{E} \parallel N_p, N_m, N_g$.)

Transition	$\langle f_{asci}\rangle \times 10^6$	Transition	$\langle f_{exp}\rangle \times 10^6$	$\langle f_{asci}\rangle \times 10^6$
$^5D_0 \rightarrow {}^5D_1$	0.8	$^7F_0 \rightarrow {}^7F_6$	1.25	1.13
$^7D_2$	2.7	$^7F_1 \rightarrow {}^7F_5$	2.14	1.97
$^5L_6$	14.8	$^7F_6$	3.67	0.92
$^5G_2$	10.5	$^7F_0 \rightarrow {}^5D_1$	0.05	0.04
$^5G_4$	30.1	$^5D_2$	0.43	0.62
$^5G_6$	1.8	$^7F_1 \rightarrow {}^5D_0$	0.08	0.05
$^5D_4$	9.4	$^5D_1$	0.81	0.72
$^5H_4$	38.2	$^5D_2$	0.12	0.04
$^5H_6$	5.5	$^5D_3$	0.71	0.52
$^5F_2$	44.1	$^7F_2 \rightarrow {}^5D_0$	1.46	—
$^5F_1$	0.04	$^7F_0 \rightarrow {}^5L_6$	2.24	2.18
$^5F_4$	307.8	$^7F_1 \rightarrow {}^5L_6$	1.81	0.42

spectrum in the visible and UV for light polarization $\boldsymbol{E} \parallel N_m$).

Absorption oscillator strengths for Eu^{3+} in KGdW host crystal were determined from the measured absorption spectrum and modeled with the theory of f–f transition intensities for systems with anomalously strong configuration interaction (ASCI) [21]—see $\langle f_{exp}\rangle$ and $\langle f_{asci}\rangle$ values in table 2; the values of f were averaged over three principal light polarizations, $\boldsymbol{E} \parallel N_p$, N_m and N_g. The set of modeling parameters is $O_{d2} = 2.6$, $O_{d4} = 2.3$, $O_{d6} = 0.76$, $O_{c2} = -0.014$, $O_{c4} = -0.024$, and $O_{c6} = -0.015$ [10^{-10} cm], $\Delta_d = 42\,360$, $\Delta_{c1} = 18\,790$, $\Delta_{c2} = 26\,590$ [cm^{-1}]. Here the parameters O_{dk} and energy Δ_d correspond to excited configuration of opposite parity $4f^{N-1}5d$, while parameters O_{ck} and energies Δ_c correspond to covalent effects of excited configurations with charge transfer.

The values of $\langle f_{asci}\rangle$ were also modeled for excited-state absorption (ESA) from the $^5D_0$ state (upper laser level); see table 2. Most intense ESA processes are related to $^5D_0 \rightarrow {}^5G_4$, $^5H_4$, $^5F_2$ and $^5F_4$ transitions; corresponding peak wavelengths are 1075, 712, 629 and 610 nm.

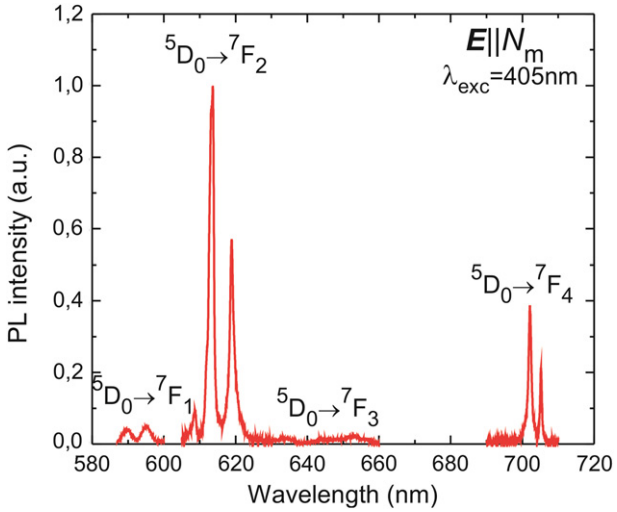

Figure 3. Photoluminescence (PL) spectrum of Eu:$KGd(WO_4)_2$ crystal for light polarization $\boldsymbol{E} \parallel N_m$ (excitation wavelength is 405 nm).

3.2. Luminescence

An overview of the photoluminescence (PL) spectrum for Eu^{3+} ions in KGdW crystal is shown in figure 3 (light polarization is $\boldsymbol{E} \parallel N_m$). The observed PL is related to radiative transitions from the $^5D_0$ state to lower-lying $^7F_{1-4}$ states. On the basis of measured polarized PL spectra, stimulated-emission cross-sections σ_{em} were determined. For this, the Fuchtbauer–Ladenburg equation [22] was utilized. Polarized stimulated-emission cross-section spectra for Eu^{3+} ions in KGdW crystal are presented in figure 4; their detailed characterization can also be found in table 1. The anisotropy of luminescent properties for Eu:KGdW is rather high. It appears both in the shape of spectral bands and in their relative intensity.

Indeed, the band associated with $^5D_0 \rightarrow {}^7F_4$ transition consists of two intense peaks centered at 702.1 and 705.2 nm (for $\boldsymbol{E} \parallel N_m$ and N_g), while for $\boldsymbol{E} \parallel N_p$ it contains one peak centered at 703.5 nm. This is in agreement with the fact that the N_p axis coincides with the C_2 symmetry axis of the DT lattice, while both N_m and N_g axes are positioned in the orthogonal plane [23]. Then, for principal light polarizations peak stimulated-emission cross-sections take the relation $\sigma_{em}(m):\sigma_{em}(p):\sigma_{em}(g) = 3.2:2.5:1$. From this point, laser crystal orientation should give access to high-gain $\boldsymbol{E} \parallel N_m$ and N_p light polarizations. For $\boldsymbol{E} \parallel N_m$, peak stimulated-emission

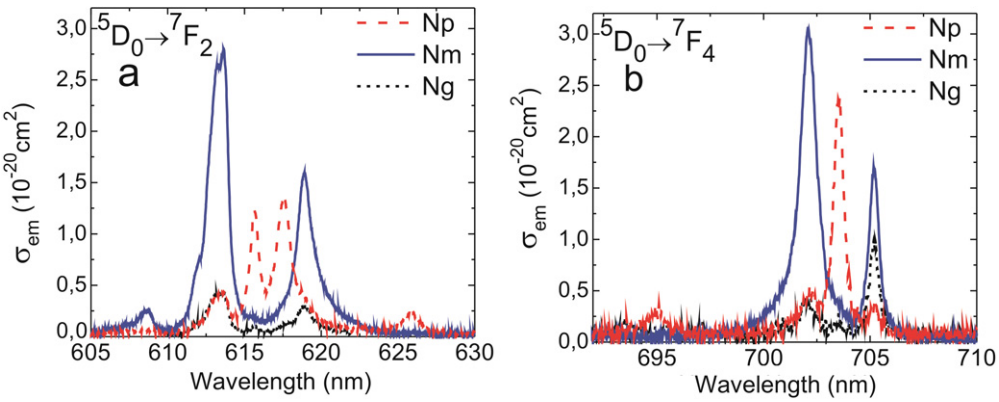

Figure 4. Polarized stimulated-emission cross-section spectra of Eu:KGd$(WO_4)_2$ crystal.

cross-section σ_{em} at the wavelength of 702.1 nm is 3.02×10^{-20} cm^2; the FWHM of this peak is ~1.1 nm.

For Eu:KGdW crystal, the band associated with $^5D_0 \rightarrow {}^7F_2$ transition overlaps with the ESA band, $^5D_0 \rightarrow {}^5F_4$. (A similar effect was observed recently for polycrystalline huntite-like $EuAl_3(BO_3)_4$ [24]). Indeed, the peak wavelength for the latter is ~610 nm (compare with figure 4(a)). Moreover, this ESA channel is the strongest (table 2). This is the main limitation for obtaining laser operation at ~612 nm with Eu:KGdW crystal.

The ratio between integral intensities of bands associated with $^5D_0 \rightarrow {}^7F_2$ (electric dipole) and $^5D_0 \rightarrow {}^7F_1$ (magnetic dipole) transitions is defined as the asymmetry parameter R [25]. It is related to the symmetry of the site of Eu^{3+} ions. An increase of the R value (dominant electric dipole $^5D_0 \rightarrow {}^7F_2$ transition) indicates increase of the crystal field strength due to increase in the covalence or in the distortion of the bonds surrounding the active ion.

According to our data, $R = 9.9$ for bulk Eu:KGdW. Previously, R was also determined for nanocrystalline Eu:KGdW (8.8–10.2 in the dependence of grain size; the content of Eu was 2 at.%) [13]. Large R values are related to (i) small average Eu–O distances in the Eu:KGdW lattice (Gd–O distances are only 2.27–2.65 Å for the host crystal); (ii) high distortion of the EuO_8 environment ($\Delta_d = 3.7 \times 10^{-3}$ for GdO_8 polyhedra) [23] and (iii) high concentration of Eu^{3+} (10 at.%) resulting in increased site distortion.

Modeling of spectroscopic properties of Eu^{3+} ion with ASCI approximation allows us to determine radiative lifetimes τ_{rad} of $^5D_0$ and $^5D_1$ states (613 and 338 μs, respectively) and luminescence branching ratios B for $^5D_0 \rightarrow {}^7F_1$, $^7F_2$ and $^7F_4$ transitions (0.08, 0.66 and 0.26, respectively).

Luminescence decay curves for KGdW crystal doped with Eu(10 at.%) are presented in figure 5. The measurements were performed at four light wavelengths, namely 595, 612, 655 and 704 nm (transitions from $^5D_0$ to $^7F_{1-4}$ states, respectively). The decay curves are clearly single exponential. Luminescence decay time τ_{exp} equals 500 ± 10 μs. This is consistent with the value obtained in [9] for Eu(25 at.%):KGdW(460 ± 10 μs).

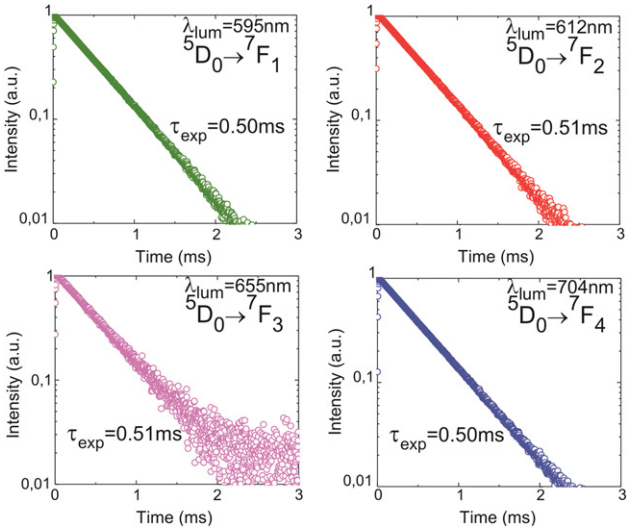

Figure 5. Luminescence decay curves for Eu:KGd$(WO_4)_2$ crystal (excitation wavelength is 405 nm).

3.3. Pulsed laser operation

Lasing was realized at $^5D_0 \rightarrow {}^7F_2$ transition (the laser wavelength was ~702.8 nm) with laser pumping at 533.6 nm into the $^7F_1 \rightarrow {}^5D_1$ absorption band of Eu^{3+} ions. Two ***b***-cut crystals, namely 10 mm-long Eu(25 at.%):KGdW and 25 mm-long Eu(10 at.%):KGdW were tested. The transversal dimensions of both crystals were 4×4 mm^2. The choice of crystals with such lengths is explained by two reasons. First, since as noted above N_{Eu} is 6.09 or 15.3×10^{20} cm^{-3}, the laser crystals used had almost the same number of active centers: 2.436×10^{20} for Eu(10 at.%):KGdW and 2.448×10^{20} for Eu(25 at.%):KGdW. Second, the excitation efficiency defined as the product of pump light absorption and quantum defect was also almost the same for both media, 72% and 70%, accordingly.

The faces of the crystals were antireflection (AR) coated for both pump and laser radiation. The crystals were placed inside the laser cavity formed by a concave input mirror with radius of curvature $R = 502$ mm and a flat output coupler with reflectivity $R_{OC} \sim 98\%$. The total cavity length was

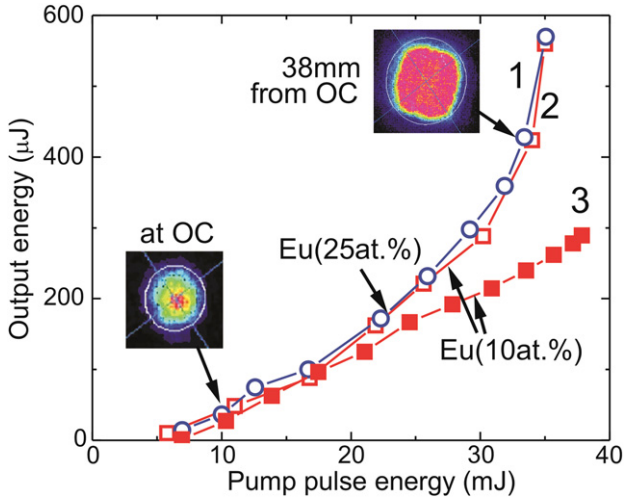

Figure 6. Output–input dependences for pulsed Eu:$KGd(WO_4)_2$ lasers; insets represent spatial profiles of the output laser beam.

35 mm. The pumping was longitudinal; a spherical lens with a focal length of 85 mm was used to focus the pump radiation. In order to avoid optical damage, Eu:KGdW crystals were positioned behind the pump beam waist. Laser crystals were passively cooled (lasing was obtained at room temperature).

Due to the above mentioned reasons, both Eu(10 at.%): and Eu(25 at.%):$KGd(WO_4)_2$ lasers have practically the same dependence of free-running lasing energy E_g on the pump pulse energy E_p (figure 6, see curves 1 and 2). The measurements of $E_g(E_p)$ dependence were performed with gradual reduction of E_p energy. The time interval between flashes has not exceeded 2 min. At $E_p = 35$ mJ, output energy E_g reaches 570 μJ and optical-to-optical laser efficiency is 1.6%. Dependence 3 was obtained for the Eu(10 at.%):KGdW laser after a long period of operation (more than 10^3 shots). The possible explanations of nonlinear behavior of output–input dependence are heat generation or formation of color centers in crystals under laser excitation. Under-air cooling, the influence of thermal effects on the operation of the Eu:KGdW laser is negligible if the energy E_p does not exceed 20 mJ. It should be noted that at the same length of crystals (10 mm), the threshold for the Eu(10 at.%):KGdW laser is approximately seven times larger (as compared with the Eu(25 at.%):KGdW one).

For both Eu:KGdW lasers, the polarization of the output beam was naturally selected ($\boldsymbol{E} \parallel N_m$). Near the threshold, the Eu(25 at.%):KGdW laser operates at the slightly elliptic TEM_{00} mode (figure 6). The beam propagation ratio in this case is $M^2 = 1.2$. It should be noted that the pump beam was elliptical and at the entrance of the Eu:KGdW crystal its principal diameters were 0.85 and 1.2 mm. Calculations of the Gaussian beam diameter at the output coupler by the ABCD matrix approach with thermal lens effect show that the flat-ended Eu:KGdW has a focal length of -1.25 m. As the average size of the pump beam for Eu(10 at.%):KGdW crystal was slightly larger (due to its length), several high-order transverse modes were observed in the laser output near the threshold. In this case, the M^2 factor was measured to be ~4. The fundamental mode operation is reached by mode selection (Eu(10 at.%):KGdW crystal was moved across the pump beam so that its waist was close to the side surface of the crystal).

As the pump energy is increased, the energy of both lasers spills out into the higher order modes. Far from laser threshold ($E_p = 25$–35 mJ), the high number of transverse modes results in good homogeneity of the output beam (figure 6). The duration of free-running pulses was 10–15 μs.

Finally, it should be noted that preliminary experiments for obtaining quasi-continuous lasing with Eu:KGdW were performed. The generation of ms long pulses with a duty cycle of 10% was reached [26]. Results will be presented in a subsequent paper.

4. Conclusions

$KGd(WO_4)_2$ crystals doped with Eu^{3+} (10, 25 at.%) are grown by the TSSG method. Their absorption spectra are studied in detail (for principal light polarizations, $\boldsymbol{E} \parallel N_p$, N_m and N_g). It is accompanied by determination of absorption oscillator strengths by means of the theory of f–f transition intensities for systems with anomalously strong configuration interaction. Spectral and temporal characteristics of luminescence associated with $^5D_0 \rightarrow {}^7F_{1-4}$ transitions are analyzed, and luminescence branching ratios and the radiative lifetime of the $^5D_0$ state are determined. Polarized stimulated-emission cross-section spectra are evaluated for Eu:KGdW. The output performance of pulsed Eu(10 at.%): and Eu(25 at.%):KGdW lasers operating at room temperature at the wavelength of 702.8 nm ($^5D_0 \rightarrow {}^7F_4$ transition) is compared under laser pumping at 533.6 nm. Both 25 mm-long Eu(10 at.%):KGdW and 10 mm-long Eu(25 at.%):KGdW provide the same output–input characteristics. The nonlinear behavior of output–input dependence is explained by heat generation or the formation of color centers in crystals under laser excitation. The influence of thermal effects in Eu:KGdW is negligible for a pump pulse energy below 20 mJ. The main limitation for laser operation at $^5D_0 \rightarrow {}^7F_2$ transition is strong excited-state absorption via the $^5D_0 \rightarrow {}^5F_4$ channel.

Acknowledgments

This work was performed within a join project of BRFBR and SB of RAS (No. F12SO-002).

References

[1] Wakefield G, Holland E, Dobson P J and Hutchison J L 2001 *Adv. Mater.* **13** 1557–60
[2] Jones S L, Kumar D, Singh R K and Holloway P H 1997 *Appl. Phys. Lett.* **71** 404–6
[3] Heikenfeld J, Garter M, Lee D S, Birkhahn R and Steckl A J 1999 *Appl. Phys. Lett.* **75** 1189–91
[4] Nyein E E, Hommerich U, Heikenfeld J, Lee D S, Steckl A J and Zavada J M 2003 *Appl. Phys. Lett.* **82** 1655–7
[5] Chang N C 1963 *J. Appl. Phys.* **34** 3500–4
[6] Schimitschek E J 1963 *Appl. Phys. Lett.* **3** 117–8

[7] Park J H and Steckl A J 2004 *Appl. Phys. Lett.* **85** 4588–90
[8] Nakamura K, Hasegawa Y, Kawai H, Yasuda N, Kanehisa N, Kai Y, Nagamura T, Yanagida S and Wada Y 2007 *J. Phys. Chem.* A **111** 3029–37
[9] Bagaev S N, Dashkevich V I, Orlovich V A, Vatnik S M, Pavlyuk A A and Yurkin A M 2011 *Quantum Electron.* **41** 189–92
[10] Pollnau M, Romanyuk Y E, Gardillou F, Borca C N, Griebner U, Rivier S and Petrov V 2007 *IEEE J. Sel. Top. Quantum Electron.* **13** 661–71
[11] Petrov V, Pujol M C, Mateos X, Silvestre O, Rivier S, Aguilo M, Sole R M, Liu J, Griebner U and Diaz F 2007 *Laser Photon. Rev.* **1** 179–212
[12] Pujol M C, Carvajal J J, Mateos X, Sole R, Massons J, Aguilo M and Diaz F 2013 *J. Lumin.* **138** 77–82
[13] Pazik R, Zych A and Strek W 2010 *Mater. Chem. Phys.* **115** 536–40
[14] Macalik L, Tomaszewski P E, Lisiecki R and Hanuza J 2008 *J. Solid State Chem.* **131** 2591–600
[15] Galceran M, Pujol M C, Gluchowski P, Strek W, Carvajal J J, Mateos X, Aguilo M and Diaz F 2010 *Opt. Mater.* **32** 1493–500
[16] Lukowiak A, Wiglusz R J, Pazik R, Lemanski K and Strek W 2008 *J. Rare Earths* **27** 564–8
[17] Gao X, Wang Y, Wang D and Liu B 2009 *J. Lumin.* **129** 840–3
[18] Klevtsov P V, Kozeeva L P and Kharchenko L Yu 1975 *Sov. Phys.—Crystallogr.* **20** 732–5
[19] Pavlyuk A A, Vasiliev Ya V, Kharchenko L Yu and Kuznetsov F A 1993 *APAM: Proc. Asia-Pacific Society for Advanced Materials* pp 164–71
[20] Binnemansy K and Gorller-Walrand C 1997 *J. Phys.: Condens. Matter* **9** 1637–48
[21] Dunina E B, Kornienko A A and Fomicheva L A 2008 *Cent. Eur. J. Phys.* **6** 407–14
[22] Aull B F and Jenssen H P 1982 *IEEE J. Quantum Electron.* **18** 925–30
[23] Pujol M C, Sole R, Massons J, Gavalda J, Solans X, Zaldo C, Diaz F and Aguilo M 2001 *J. Appl. Crystallogr.* **34** 1–6
[24] Malashkevich G E, Kornienko A A, Dunina E B, Sigaev V N, Golubev N V, Mamadjanova E H and Paleary A 2013 *J. Appl. Spectrosc.* at press
[25] Kirby A F and Richardson F S 1983 *J. Phys. Chem.* **87** 2544–56
[26] Loiko P A, Dashkevich V I, Bagaev S N, Orlovich V A, Yasukevich A S, Yumashev K V, Kuleshov N V, Vatnik S M and Pavlyuk A A 2013 *Proc. CLEO/Europe-EQEC 2013 (Munich, May 2013)* p CA-2.3